



Microstructures and electrical responses of pure and chromium-doped $\text{CaCu}_3\text{Ti}_4\text{O}_{12}$ ceramics

Qian Zheng, Huiqing Fan*, Changbai Long

State Key Laboratory of Solidification Processing, School of Materials Science and Engineering, Northwestern Polytechnical University, Xi'an 710072, China

ARTICLE INFO

Article history:

Received 8 August 2011

Received in revised form 3 September 2011

Accepted 5 September 2011

Available online 10 September 2011

Keywords:

CCTO ceramics

Microstructure

Grain boundaries

Electronic properties

ABSTRACT

Pure and chromium-doped CCTO ($\text{CaCu}_3\text{Ti}_4\text{O}_{12}$) ceramics were prepared by a conventional solid-state reaction method, and the effects of chromium doping on the microstructures and electrical properties of these ceramics were investigated. Efficient crystalline phase formation accompanied by dopant-induced lattice constant expansion was confirmed through X-ray diffraction studies. Scanning electron microscopy (SEM) results show that doping effectively enhanced grain growth or densification, which should increase the complex permittivity. The dielectric constant reached a value as high as 20,000 (at 1 kHz) at a chromium-doping concentration of 3%. The electrical relaxation and dc conductivity of the pure and chromium-doped CCTO ceramics were measured in the 300–500 K temperature range, and the electrical data were analyzed in the framework of the dielectric as well as the electric modulus formalisms. The obtained activation energy associated with the electrical relaxation, determined from the electric modulus spectra, was 0.50–0.60 eV, which was very close to the value of the activation energy for dc conductivity (0.50 ± 0.05 eV). These results suggest that the movement of oxygen vacancies at the grain boundaries is responsible for both the conduction and relaxation processes. The short-range hopping of oxygen vacancies as “polarons” is similar to the reorientation of the dipole and leads to dielectric relaxation. The proposed explanation of the electric properties of pure and chromium-doped CCTO ceramics is supported by the data from the impedance spectrum.

© 2011 Elsevier B.V. All rights reserved.

1. Introduction

Recently, there has been considerable interest in materials having high dielectric constants, because such materials might offer the opportunity to enhance the performance or shrink the dimensional sizes of fabricated devices. High dielectric constants are usually found in ferroelectric materials and are related to atomic displacements within a non-centrosymmetric structure. $\text{CaCu}_3\text{Ti}_4\text{O}_{12}$ (CCTO), which has a cubic perovskite-related crystal structure, is an attractive material with an unusual dielectric property. It exhibits a large dielectric constant of approximately 10^4 that is independent of temperature and frequency below 10^6 Hz at room temperature in both the single crystalline and ceramic forms [1,2]. Furthermore, structural studies have indicated that CCTO does not show any phase transitions down to temperatures as low as 35 K [3–5].

Till now, the underlying operative mechanisms of the giant dielectric response in these systems are not well established. Some researchers reported that the high dielectric constant behavior should be attributed to local dipole moments associated with off center displacement of Ti ions [6]. While others prefer to attribute it to some extrinsic factors, such as the material microstructure (such

as grain size) [7,8], processing conditions (such as sintering temperature and time, cooling rate, etc.) [7–9], twin crystals [1], an internal barrier layer capacitance (IBLC) model in which the ceramic is supposed to consist of n-type semiconductive grains and insulating grain or domain boundaries [5,10,11], internal domains inside CCTO grains [11,12], electrode polarization effects [13], a multipole trap charge repositioning model [14,15] and so on. Contact electrode depletion effect [13] and other similar behavior termed Maxwell–Wagner relaxation [16] were also proposed and generally accepted.

In this study, the influences of Cr ion doping on the microstructures and dielectric properties of CCTO were investigated. We focus on the variations in the electrical modulus spectra with the intent of exploring the influences of chromium (Cr) doping on the electrical properties of CCTO; this study is expected to provide new insights into deciphering the physical origin of the anomalous dielectric responses of CCTO and rationalizing the electrical behavior of these ceramics.

2. Experimental procedure

Pure and Cr-doped CCTO ceramics were prepared by solid-state reaction. The raw materials were the analytical grade powders of CaCO_3 , CuO, TiO_2 and Cr_2O_3 , which leads to the chemical formula $\text{CaCu}_3\text{Ti}_{4-x}\text{Cr}_x\text{O}_{12-x/2}$ ($x=0, 0.01, 0.02, 0.03$, abbreviated as CCTC-0, CCTC-1, CCTC-2 and CCTC-3, respectively). Calculated quantities of the raw materials were wet ball-milled using ethanol as a solvent for 12 h.

* Corresponding author. Tel.: +86 29 88494463; fax: +86 29 88492642.

E-mail address: hqfan3@163.com (H. Fan).

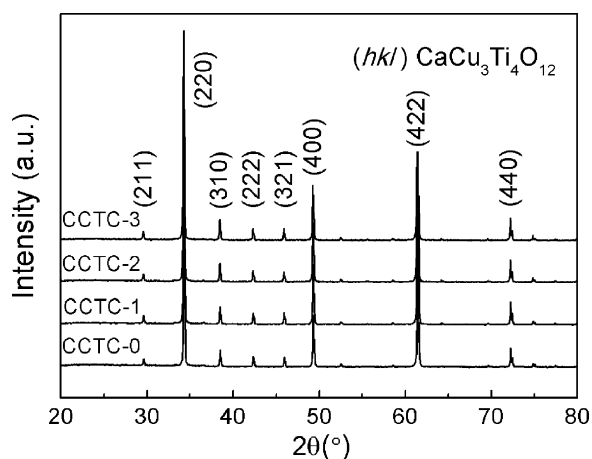


Fig. 1. X-ray diffraction patterns of $\text{CaCu}_3\text{Ti}_{4-x}\text{Cr}_x\text{O}_{12-x/2}$ ceramics ($x=0, 0.01, 0.02,$ and 0.03) sintered at 1070°C for 6 h.

The dried mixtures were then calcined at 950°C for 6 h in an alumina crucible and then furnace cooled. The calcined powders were ground for 12 h in ethanol and then were pressed into pellets of 12 mm diameter and 1 mm thickness at a pressure of 250 MPa using a cold isostatic press. The pellets were sintered in air at 1070°C for 6 h and cooled naturally to room temperature.

The crystalline phase of all samples was examined using X-ray diffraction (XRD; X'pert PRO MPD, Philips, Eindhoven, Netherlands) with $\text{Cu K}\alpha$ radiation with an applied voltage of 40 kV and current of 500 mA. The XRD data for Rietveld analysis were collected over the range of $2\theta=20^\circ\text{--}120^\circ$ with a step size of 0.02° and a count time of 2 s. The microstructure of the ceramics was investigated using a scanning electron microscopy with an applied voltage of 15 kV (SEM; Model JEOL-6700F, Japan Electron Co., Tokyo, Japan). The sintered bulk density ρ was measured by the Archimedes method. For the electrical property measurements, silver paste was painted on the polished pellets as the electrodes and fired at 550°C for 20 min. The dielectric properties and impedance spectra were measured using a frequency response analyzer (4294A, Agilent, CA, USA) at a signal amplitude of 500 mV/mm in the frequency range from 100 Hz to 1 MHz and the dc electric conductivity as a

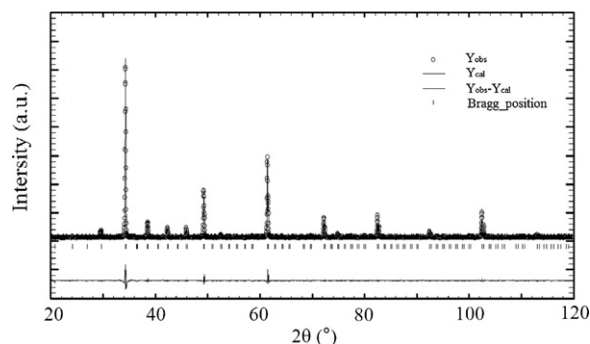


Fig. 2. Profile fits for the Rietveld refinement of $\text{CaCu}_3\text{Ti}_{4-x}\text{Cr}_x\text{O}_{12-x/2}$ ceramics.

function of temperature was carried out by using a high resistance meter (4339B, Agilent, CA, USA) associated with component test fixture (16339A, Agilent, CA, USA) in conjunction with a temperature controller (TP94, Linkam, Surrey, UK) at the heating rate of $3^\circ\text{C}/\text{min}$.

3. Results and discussions

Fig. 1 shows the XRD patterns of sintered pure and Cr-doped CCTO ceramics with different doping concentrations. All the diffraction peaks appeared in the patterns matched with the peaks of the pseudo-cubic CCTO by comparing with the standard powder diffraction file database (JCPDF File No. 75-2188), with no traces from other impurity phases, indicating that a solid solution has been formed. The profile fits of the Rietveld refinement for the $\text{CaCu}_3\text{Ti}_{4-x}\text{Cr}_x\text{O}_{12-x/2}$ ($x=0.03$) ceramic was shown in **Fig. 2**. The refinements were carried out in the cubic space group $\text{Im}\bar{3}$ by using the software FULLPROF. The final weighted residue factor R_{wp} and the goodness of fit S (R_{wp}/R_{exp}) were 10.6% and 1.59. These refinement parameters were reasonable values, indicating

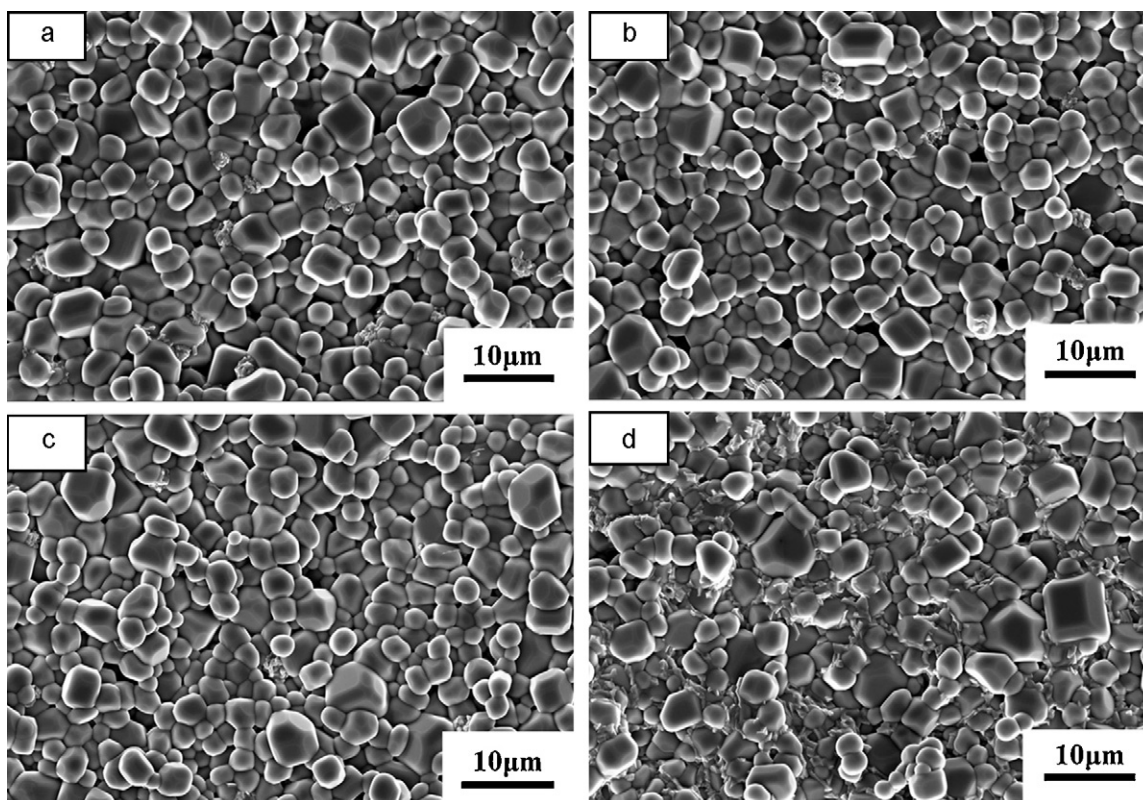


Fig. 3. Scanning electron microscopy graphs of $\text{CaCu}_3\text{Ti}_{4-x}\text{Cr}_x\text{O}_{12-x/2}$ ceramics (a) $x=0$, (b) $x=0.01$, (c) $x=0.02$ and (d) $x=0.03$ sintered at 1070°C for 6 h.

Table 1
Lattice parameter (a), density (ρ) and mean grain size (D) of the samples.

Samples	a (Å)	ρ (g/cm ³)	D (μm)
CCTC-0	7.382(3)	4.49 ± 0.05	2.59 ± 0.5
CCTC-1	7.385(1)	4.42 ± 0.02	2.37 ± 0.6
CCTC-2	7.389(4)	4.50 ± 0.01	2.64 ± 0.3
CCTC-3	7.390(8)	4.57 ± 0.02	3.62 ± 0.7

the reliability of the refined structural parameters. In addition, the refinements were performed on the basis of the assumption that Cr ions substituted Ti occupied on B sites at perovskite structure. The structural parameters obtained by Rietveld refinement clearly indicated that Cr ions indeed entered the lattice site for Ti. The lattice parameter increased with increasing Cr substitution, these refined lattice parameters were $a = 7.382(3)$ Å, $a = 7.385(1)$ Å, $a = 7.389(4)$ Å, $a = 7.390(8)$ Å for CCTC-0, CCTC-1, CCTC-2 and CCTC-3, respectively, which were shown in Table 1.

Fig. 3 shows the SEM microstructures of the CCTO ceramics as a function of chromium concentration. At Cr dopant contents (x) up to 0.02, loosely linked grains having clear a grain boundary and a mean grain size ranging from 2 to 3 μm are observed along with some holes. SEM images indicate that very little microstructural difference between the pure CCTO and the doped pellets. However, as the Cr doping content is increased up to $x = 0.03$, there is a further increase in the mean grain size to approximately 4 μm (Table 1) with no clear grain boundary. The density of the pellets was measured using the Archimedes method. It can be seen that the density increases to reach a value of 4.57 g/cm³ as the chromium concentration increases (Table 1). The effects of variations in the microstructural characteristics were evaluated by monitoring the dielectric properties of the various Cr-doped CCTO ceramics.

Fig. 4 illustrates the real (ϵ') and imaginary (ϵ'') parts of dielectric constant as function of frequency and chromium content. A clear relationship can be seen between chromium amount and dielectric constant or loss. In general, all the pellets show giant dielectric constant values ($>10^4$) in a broad frequency range. The highest doped pellets showed highest dielectric constants (2×10^4) over the whole frequency range, meanwhile, these pellets presented even the highest dielectric loss. This behavior maybe attributed to differences on the grain size, according to the internal boundary layer capacitance (IBLC) model, the effective dielectric constant is inversely proportional to the ratio of thickness of the insulating layer (i.e. grain boundary) to the grain size. The observed increased dielectric constant for the bigger-grained Cr-substituted pellets may arise due to the change in the grain boundary thickness [8]. In addition, during the sintering process, trivalent element Cr can act as an acceptor dopant to substitute Ti which is likely to occur in CCTO grains, because the radius of Cr³⁺ (0.615 Å) is larger than that of Ti⁴⁺ (0.605 Å), this can be confirmed by the increase of the lattice parameter [17]. Meanwhile, it would give rise to cations defects or oxygen vacancies in grain boundary regions resulting in higher conductivity, it will also impact on the dielectric properties.

In order to elucidate the electrical transport mechanism in the Cr-doped CCTO ceramics, the electric modulus approach was analyzed. The phenomenological nature of the electric modulus [18] is used to invoke the relaxation processes of ions in these materials. This approach can effectively be employed to study bulk electrical behavior of the moderately conducting pellets. The complex electric modulus (M^*) is defined in terms of the complex dielectric constant (ϵ^*) and is represented as

$$M^* = (\epsilon^*)^{-1} \quad (1)$$

$$M' + iM'' = \frac{\epsilon'}{(\epsilon')^2 + (\epsilon'')^2} + i \frac{\epsilon''}{(\epsilon')^2 + (\epsilon'')^2} \quad (2)$$

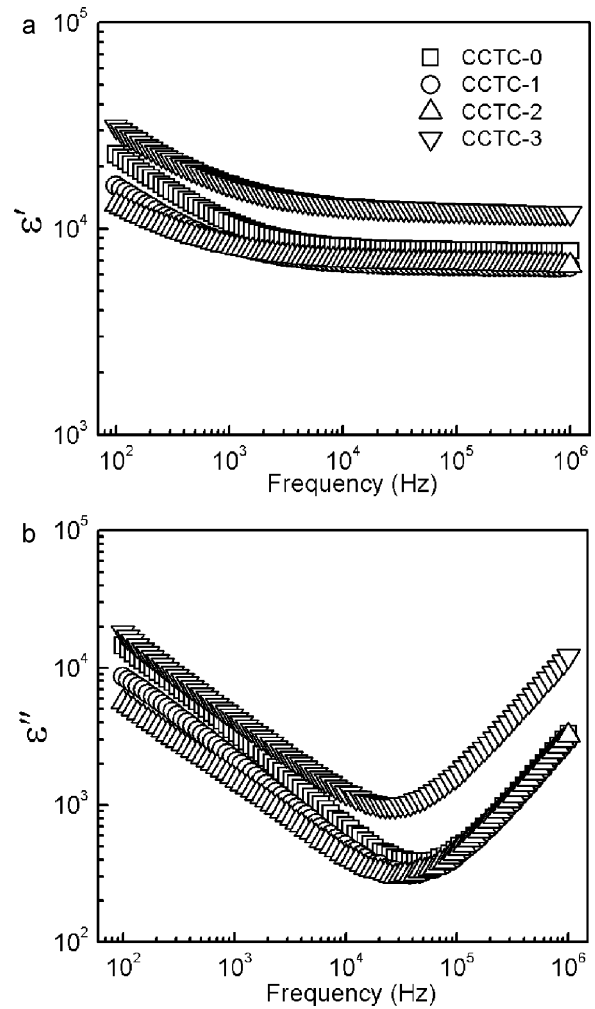


Fig. 4. Frequency dependence of (a) the real ϵ' and (b) and imaginary ϵ'' parts of dielectric constant of pure and chromium doped $\text{CaCu}_3\text{Ti}_{4-x}\text{Cr}_x\text{O}_{12-x/2}$ ceramics measured at room temperature.

where M' , M'' and ϵ' , ϵ'' are the real and imaginary parts of the electric modulus and dielectric constants, respectively. The imaginary parts of the modulus at various temperatures are calculated using Eq. (2) for the Cr-doped CCTO ceramics and depicted in Fig. 5. It can be seen that the M'' peak shifts to higher frequencies with increasing temperature in the 10^2 – 10^6 Hz range for each pellet, indicating the involvement of a temperature-dependent Debye relaxation processes. These Debye processes that appear at intermediate frequencies can be attributed to a grain boundary response [19]. The grain boundary relaxation time is large, which suggests that the grain boundary plays a crucial role in determining the electronic property. Fig. 5 reveals the relaxation nature of the thermally activated process, and thus, the activation energy can be deduced from this shift by the Arrhenius law [20]:

$$\tau = \tau_0 \exp\left(-\frac{E_{\text{relax}}}{k_B T}\right) \quad (3)$$

where τ is the relaxation time, τ_0 is the pre-exponential factor and E_a is the activation energy. Fig. 6 shows $\ln(\tau)$ as a function of the inverse of the M'' peak temperature T ; the solid lines represent the results fitted using Eq. (3). The relaxation time and the activation energies of the dielectric relaxations were calculated from the slopes of the fitted straight lines, and the data are listed in Table 2. The activation energy values fell within the range of $E_a = 0.50$ – 0.60 eV, which are very close to the value

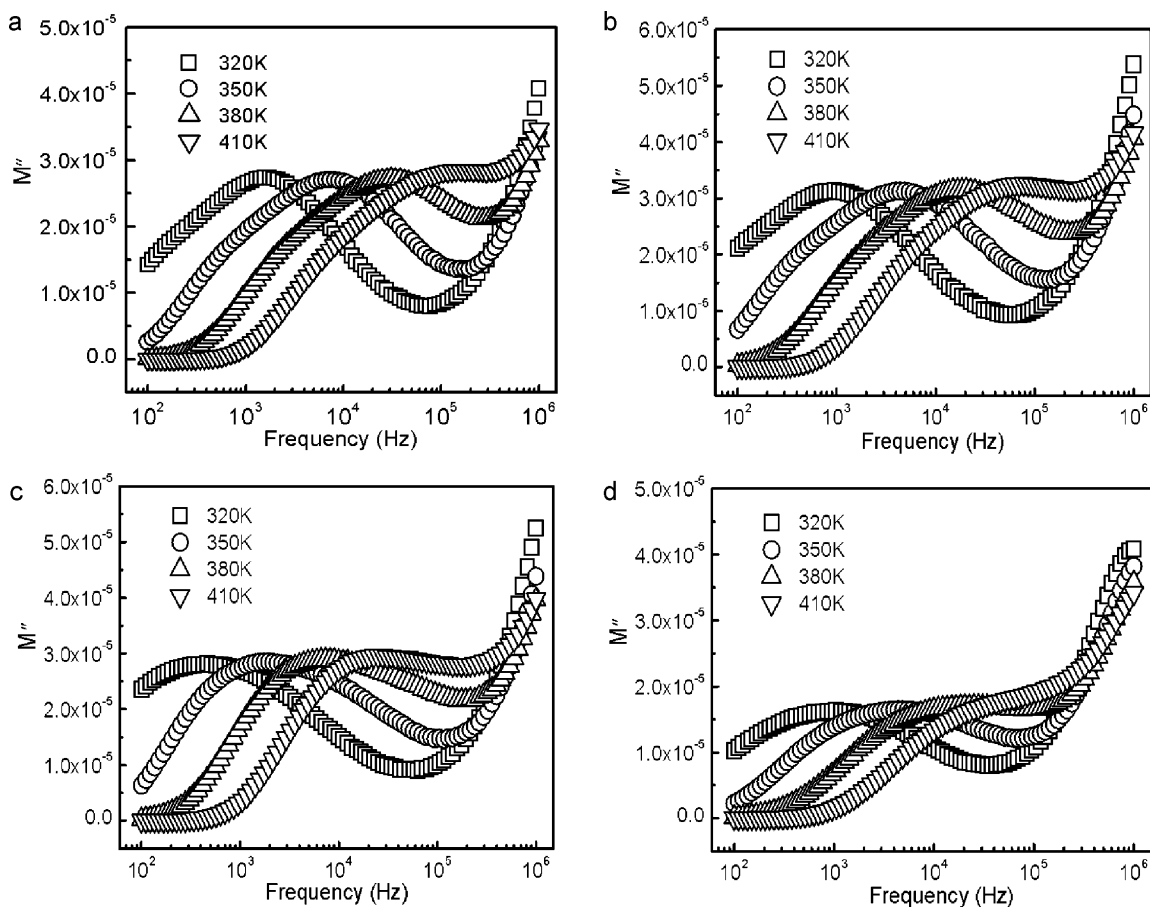


Fig. 5. Frequency dependence of imaginary parts of the electric modulus at various temperatures of $\text{CaCu}_3\text{Ti}_{4-x}\text{Cr}_x\text{O}_{12-x/2}$ ceramics (a) $x=0$, (b) $x=0.01$, (c) $x=0.02$, (d) $x=0.03$.

of ~ 0.54 eV reported by Zhang for the extrinsic grain boundary Maxwell–Wagner relaxation [21]. We attribute the obtained energies to the activation of oxygen vacancies. The oxygen vacancies and space charges (electrons) are produced in the grain boundaries. The relaxation time of the ceramics is reported to be approximately in the range of 10^{-10} – 10^{-13} s, which is related to the attempt frequency of ion hopping [22]. Owing to the inhibition of long-range motions of the oxygen vacancies by the grain boundary, the relaxation process can be attributed to short-range hopping, similar to the reorientation of the dipole.

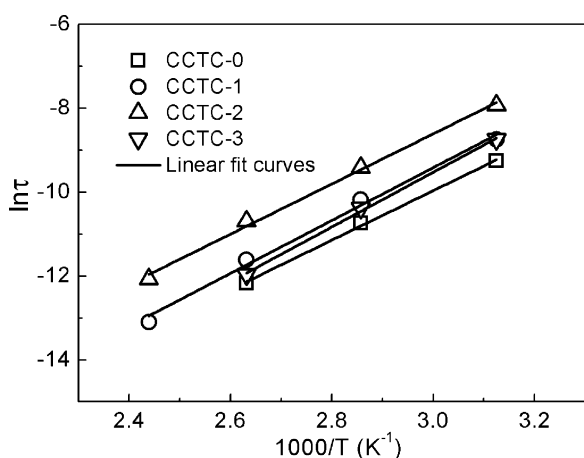


Fig. 6. Temperature dependence of the relaxation time τ ($\ln \tau$ versus $1000/T$) for dielectric relaxation.

Using a space-charge model, Bidault et al. found that the localization of free charges at the metal dielectric interface is responsible for the low-frequency dielectric relaxation in several perovskite materials containing titania. A correlation between the dielectric relaxation and the conductivity has also been established—an increase in the oxygen vacancies leads to an increase in both the conductivity and the dielectric relaxation [23]. Fig. 7 illustrates $\ln(\sigma_{\text{dc}})$ versus $1000/T$ for the Cr-doped CCTO ceramics. The plot is found to be linear and fitted using following Arrhenius equation:

$$\sigma_{\text{dc}} = \sigma_0 \exp\left(-\frac{E_{\text{dc}}}{k_{\text{B}}T}\right) \quad (4)$$

where σ_0 is the pre-exponential factor, E_{dc} is the activation energy for the dc conduction, k_{B} the Boltzmann constant, and T the absolute temperature. The calculated activation energy was 0.46 eV, 0.47 eV, 0.50 eV and 0.45 eV, respectively, for the CCTC-0, CCTC-1, CCTC-2 and CCTC-3 ceramics. These direct conduction activation energies are not far from 0.70 eV, which is the conduction activated energy of the electrons from the second ionization of oxygen vacancies [24]. These data give some hints that the dielectric relaxation in the Cr-doped CCTO ceramics may be related to the point defects (oxygen vacancies or space charges) in the grain boundaries. Meanwhile, these values for activation energy are in close agreement with the activation energy for electrical relaxation. Hence, it is reasonable

Table 2
Curve fitting results for the chromium doped $\text{CaCu}_3\text{Ti}_{4-x}\text{Cr}_x\text{O}_{12-x/2}$ ceramics.

Samples	CCTC-0	CCTC-1	CCTC-2	CCTC-3
τ_0 (s)	0.97×10^{-12}	0.50×10^{-12}	0.29×10^{-11}	0.23×10^{-12}
E_a (eV)	0.51	0.54	0.52	0.56

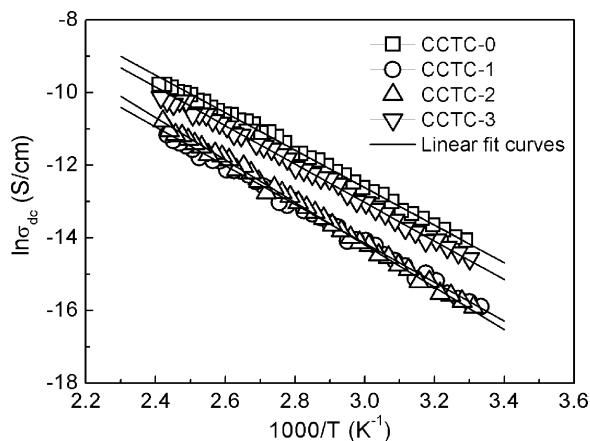


Fig. 7. Temperature dependence of the dc conductivity σ_{dc} ($\ln \sigma_{dc}$ versus $1000/T$) for pure and chromium doped $\text{CaCu}_3\text{Ti}_{4-x}\text{Cr}_x\text{O}_{12-x/2}$ ceramics.

to assume that the localized oxygen vacancies act as “polarons,” leading to a dielectric relaxation in the Cr-doped CCTO ceramics.

In order to further observe the dielectric response of grain and grain boundary of the Cr-doped CCTO ceramics, complex impedance (Z^*) plots were analyzed. Fig. 8 shows the Cole–Cole impedance plots at 350 K in the 100 Hz to 10 MHz frequency range. The experimental impedance data only cover a part of the semicircles or arcs because of the limit of the measured frequency range. Only a fraction of the grain boundary arc is observed in all pellets, which is composed of a resistor and a capacitor joined in parallel. It can be seen that the addition of Cr has influence on the resistivity of R_g and R_{gb} , especially for the grain boundary. The non-zero intercept on the Z' axis gives the grain (R_g) value and grain boundary (R_{gb}) value may also be directly obtained by the other intercept on the Z' axis from the low-frequency impedance data. The bulk resistance of pellets are $\sim 90, 96, 100$ and $82 \Omega \text{ cm}$ corresponding to CCTC-0, CCTC-1, CCTC-2 and CCTC-3 ceramics, respectively. From Fig. 8, it can be observed that the R_g and R_{gb} first increased with the increasing of Cr doping concentration, and then the R_g and R_{gb} are abruptly decreased when the Cr doping concentration exceeds a certain value (about 2%). This phenomenon suggests that the chromium as acceptor dopant influences the resistance of the grain and the grain boundary by producing oxygen vacancies [25], which result in that the turning points of electrical properties occur at a certain doping concentration. The fact that the dielectric

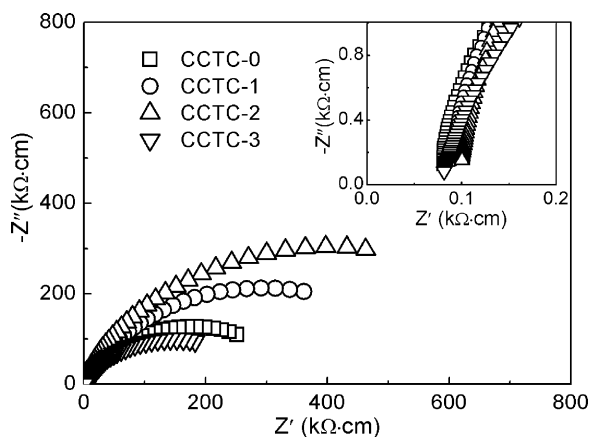


Fig. 8. Impedance complex plane plots of the chromium doped $\text{CaCu}_3\text{Ti}_{4-x}\text{Cr}_x\text{O}_{12-x/2}$ ceramics at 350 K. The inset shows an expanded view of the high frequency data close to the origin.

constant abruptly increases when the Cr doping concentration exceeds 2% may be due to the increase of grain size.

4. Conclusions

Pure and chromium-doped CCTO ceramics were produced using the solid-state reaction method, and the effects of chromium doping on the microstructures and electrical properties of the CCTO ceramics were investigated. SEM analysis indicates that doping enhanced the grain growth or densification, which increases the complex permittivity. The dielectric properties of the pure and chromium-doped CCTO ceramics were rationalized by using the electric modulus formalism. The relaxation behavior at intermediate frequencies may be explained by the modified temperature-dependent Debye equation. The value of the activation energy associated with the relaxation (0.50–0.60 eV) was very close to that of the activation energy for dc conductivity (0.50 ± 0.05 eV), which suggests that the movements of oxygen vacancies at the grain boundaries are responsible for both the conduction and relaxation processes. The short-range hopping of oxygen vacancies as “polarons” with $\tau_0 = 0.97 \times 10^{-12} - 0.29 \times 10^{-11}$ s is similar to the reorientation of the dipole and leads to dielectric relaxation, whereas long-range motion is inhibited by the grain boundary with increasing chromium content. The results of impedance measurements corroborate these inferences.

Acknowledgements

This work was financially supported by the National Nature Science Foundation (51172187), the SRPDF and 111 Program (B08040) of MOE, the Xi'an Science and Technology Foundation (XA-AM-201003), the NPU Doctoral Foundation (CX-201006) and the SKLSP Research Fund (40-QZ-2009) of China.

References

- [1] M.A. Subramanian, D. Li, N. Duan, B.A. Reisner, A.W. Sleight, J. Solid State Chem. 151 (2000) 323–325.
- [2] A.P. Ramirez, M.A. Subramanian, M. Gardel, G. Blumberg, D. Li, T. Vogt, S.M. Shapiro, Solid State Commun. 115 (2000) 217–220.
- [3] C.C. Homes, T. Vogt, S.M. Shapiro, S. Wakimoto, A.P. Ramirez, Science 293 (2001) 673–675.
- [4] M.A. Subramanian, A.W. Sleight, Solid State Sci. 4 (2002) 347–351.
- [5] D.C. Sinclair, T.B. Adams, F.D. Morrison, A.R. West, Appl. Phys. Lett. 80 (2002) 2153–2155.
- [6] S.M. Ke, H.T. Huang, H.Q. Fan, Appl. Phys. Lett. 89 (2006) 182904.
- [7] T. Li, Z. Chen, Y. Su, L. Su, J. Zhang, J. Mater. Sci. 44 (2009) 6149–6154.
- [8] V. Brizé, G. Gruener, J. Wolfman, K. Fatyeyeva, M. Tabellout, M. Gervais, F. Gervais, Mater. Sci. Eng. B 129 (2006) 135–138.
- [9] C.M. Wang, S.Y. Lin, K.S. Kao, Y.C. Chen, S.C. Weng, J. Alloys Compd. 491 (2010) 423–430.
- [10] L.J. Liu, H.Q. Fan, P.Y. Fang, X.L. Chen, Mater. Res. Bull. 43 (2008) 1800–1807.
- [11] T.T. Fang, C.P. Liu, Chem. Mater. 17 (2005) 5167–5171.
- [12] J.L. Zhang, P. Zheng, C.L. Wang, Appl. Phys. Lett. 87 (2005) 142901.
- [13] P. Lunkenheimer, R. Fichtl, S.G. Ebbinghaus, A. Loidl, Phys. Rev. B 70 (2004) 172102.
- [14] X.J. Luo, C.P. Yang, S.S. Chen, X.P. Song, H. Wang, K. Baerner, J. Appl. Phys. 108 (2010) 014107.
- [15] K. Baerner, X.J. Luo, X.P. Song, C. Hang, S.S. Chen, I.V. Medvedeva, C.P. Yang, J. Mater. Res. 26 (2011) 36–44.
- [16] W. Li, R.W. Schwatz, Phys. Rev. B 75 (2007) 012104.
- [17] T. Li, Z.P. Chen, F.G. Chang, J.H. Hao, J.C. Zhang, J. Alloys Compd. 484 (2009) 718–722.
- [18] P.B. Macedo, C.T. Moynihan, R. Bose, Phys. Chem. Glasses 13 (1972) 171–179.
- [19] L.J. Liu, H.Q. Fan, X.L. Chen, P.Y. Fang, J. Alloys Compd. 469 (2009) 529–534.
- [20] Y.H. Lin, J.N. Cai, M. Li, C.W. Nan, J.L. He, J. Appl. Phys. 103 (2008) 074111.
- [21] L. Zhang, Appl. Phys. Lett. 87 (2005) 022907.
- [22] J.G. Hou, R. Vaish, Y.F. Qu, D. Krsmanovic, K.B.R. Varma, R.V. Kumar, Mater. Chem. Phys. 121 (2010) 32–36.
- [23] O. Bidault, P. Goux, M. Kchikech, M. Belkaoui, M. Maglione, Phys. Rev. B 49 (1994) 7868–7873.
- [24] L. Ni, X.M. Chen, Appl. Phys. Lett. 91 (2007) 122905.
- [25] M.A. Sulaiman, S.D. Hutagalung, M.F. Ain, Z.A. Ahmad, J. Alloys Compd. 493 (2010) 486–492.